blood advances®

Proteomic and bioinformatic profiling of neutrophils in CLL reveals functional defects that predispose to bacterial infections

Nirojah Subramaniam,[1,2] Jenny Bottek,[1] Stephanie Thiebes,[1] Kristina Zec,[1,3] Matthias Kudla,[1] Camille Soun,[1] Elena de Dios Panal,[1,4] Julia K. Lill,[1,5] Aaron Pfennig,[6] Ralf Herrmann,[7] Kirsten Bruderek,[8] Sven Rahmann,[6] Sven Brandau,[8] Patricia Johansson,[9] Hans Christian Reinhardt,[9] Jan Dürig,[9] Martina Seiffert,[10] Thilo Bracht,[11,12] Barbara Sitek,[11] and Daniel Robert Engel[1]

[1]Institute of Experimental Immunology and Imaging, University Hospital Essen, University Duisburg-Essen, Essen, Germany; [2]Bayer AG, Pharma Research Center, Wuppertal, Germany; [3]Kennedy Institute of Rheumatology, University of Oxford, Oxford, United Kingdom; [4]University Medical Centre Utrecht, Center for Translational Immunology, Utrecht, The Netherlands; [5]Leibniz-Institut für Analytische Wissenschaften, Leibniz-Institut für Analytische Wissenschaften (ISAS–e.V.), Dortmund, Germany; [6]Genome Informatics, Institute of Human Genetics, [7]Division of Neonatology, Kinderklinik I, University Hospital Essen, University Duisburg-Essen, Essen, Germany; [8]Research Division, Department of Otorhinolaryngology, University Hospital Essen, West German Cancer Center, Essen, Germany; [9]Department of Hematology and Stem Cell Transplantation, West German Cancer Center, German Consortium for Translational Cancer Research, University Hospital Essen, University Duisburg-Essen, Essen, Germany; [10]Molecular Genetics, German Cancer Research Center, Heidelberg, Germany; [11]Medizinisches Proteom-Center, Medical Faculty, Ruhr-University Bochum, Bochum, Germany; and [12]Klinik für Anästhesiologie, Intensivmedizin und Schmerztherapie, Universitätsklinikum Knappschaftskrankenhaus Bochum, Bochum, Germany

Key Points

- CLL represses the antibacterial function of neutrophils and increases bacterial infections.

- Progression of CLL reduces expression of CD62L and CXCR4 by neutrophils and is associated with impaired migration.

Patients with chronic lymphocytic leukemia (CLL) typically suffer from frequent and severe bacterial infections. Although it is well known that neutrophils are critical innate immune cells facilitating the early defense, the underlying phenotypical and functional changes in neutrophils during CLL remain largely elusive. Using a murine adoptive transfer model of CLL, we demonstrate aggravated bacterial burden in CLL-bearing mice upon a urinary tract infection with uropathogenic *Escherichia coli*. Bioinformatic analyses of the neutrophil proteome revealed increased expression of proteins associated with interferon signaling and decreased protein expression associated with granule composition and neutrophil migration. Functional experiments validated these findings by showing reduced levels of myeloperoxidase and acidification of neutrophil granules after ex vivo phagocytosis of bacteria. Pathway enrichment analysis indicated decreased expression of molecules critical for neutrophil recruitment, and migration of neutrophils into the infected urinary bladder was significantly reduced. These altered migratory properties of neutrophils were also associated with reduced expression of CD62L and CXCR4 and correlated with an increased incidence of infections in patients with CLL. In conclusion, this study describes a molecular signature of neutrophils through proteomic, bioinformatic, and functional analyses that are linked to a reduced migratory ability, potentially leading to increased bacterial infections in patients with CLL.

Introduction

Chronic lymphocytic leukemia (CLL), an indolent B-cell non-Hodgkin lymphoma (B-NHL), is the most frequent leukemia in the Western hemisphere.[1] The disease is characterized by the massive outgrowth of CD5^{+} B cells, which accumulate primarily in the bone marrow (BM), blood, and lymph nodes.[2] While the majority of patients with CLL experience an indolent course with unspecific symptoms, such as fatigue and fever, the clonal expansion of B cells leads to an immunocompromised state predisposing patients to bacterial infections for largely unknown reasons.[3-13] Frequent and infections often lead to the

The full-text version of this article contains a data supplement.

initial diagnosis of CLL,[14] and infection-related complications hamper adherence to chemo- or immunotherapy and pose a major threat, resulting in high morbidity and mortality rates in patients with CLL.[12,13]

Urinary tract infections (UTIs) are one of the most common and nosocomial infections, with the vast majority being caused by uropathogenic *Escherichia coli* (UPEC).[15,16] This pathogen invades the outer urothelial lining of the urinary bladder,[17] and increased frequency and incidence has been observed in patients with CLL.[18] Neutrophils are the most critical responders in acute infections of the urinary bladder. They infiltrate the infected urinary bladder and cross the basement membrane of the infected urothelium through matrix metalloproteinase 9 (MMP9).[19-21] At bacterial foci, neutrophils phagocytose UPEC,[22] and the absence of neutrophils in UTI leads to aggravated disease courses, recurrence, and tissue damage.[21,23] In patients with CLL, there is conflicting data on the functional repertoire of neutrophils,[24-29] and it remains elusive whether a particular molecular phenotype and functional defect of neutrophils predispose patients to increased risk of infections.

This study shows an increased bacterial burden in the UPEC-infected urinary bladder of CLL-bearing mice. Enrichment analysis, STRING (Search Tool for the Retrieval of Interacting Genes/Proteins) protein interaction, and a random forest classifier (RFC) revealed many alterations in the phenotype and function of neutrophils in CLL. We observed increased interferon (IFN) signaling, reduced expression of granule proteins, and impaired migration of neutrophils in CLL-bearing mice. Conclusively, a combination of bioinformatic and functional analyses identified a particular molecular signature of neutrophils in CLL with potential biomarker and target molecules.

Methods

Mice and CLL induction

Recipient mice were bred and maintained under specific-pathogen–free conditions at the animal facilities of the University Clinic Essen. Donor mice were bred and maintained at the animal facilities of the German Cancer Research Center in Heidelberg. Female C57BL/6 mice (8-12 weeks of age) were injected IV with 2×10^7 syngeneic splenocytes from C57BL/6 donor mice, which were transplanted with leukemic Eμ-TCL1 cells as previously described.[30-33] The CLL burden in mice was determined by the percentage of $CD5^+ CD19^+$ B cells in the blood by flow cytometry (FC). In order to study the susceptibility to UTIs, CLL mice with 20% $CD5^+ CD19^+$ B cells in the blood were used throughout the study. Animal experiments were approved by the local animal review board of the government (Bezirksregierung Köln, Landesamt für Natur, Umwelt und Verbraucherschutz NRW, Recklinghausen, Germany) as documented in file references 84-02.04.2015.A211 and 81-02.04.2018.A058.

Murine UTI model

The synthesis of GFP-expressing UPEC[34] and the in vivo UTI model were described in previous studies.[21,35] UPEC strain 536 (O6:K15: H31) was derived from a UTI patient.[36] GFP-expressing *E coli* 536 were cultured for 3 hours at 37°C in LB medium. Bacteria were harvested via centrifugation and suspended in sterile phosphate-buffered saline (PBS). Subsequently, animals were infected via transurethral inoculation of 5×10^8 UPEC using a soft polyethylene

catheter as previously described.[21] In order to study the susceptibility to infections, CLL mice with 20% $CD5^+ CD19^+$ B cells in the blood were used.

FC analysis

Murine blood was collected via cardiac puncture, and bladders were harvested. Human blood samples were collected in citrate vacutainers in accordance with the local ethics committee at the University Hospital Essen (reference number 14-6080-BO). After red blood cell lysis, blood samples from mice and humans were processed for subsequent antibody staining. Single-cell suspensions from bladders were obtained by enzymatic digestion in RPMI1640 (10% heat-inactivated fetal calf serum, 1 mM L-glutamine, 100 μg/mL penicillin/streptomycin, 0.5 mg/mL collagenase, and 100 μg/mL DNase I) for 45 minutes at 37°C. For cell surface staining, cell suspensions were incubated for 20 minutes at 4°C with antibodies. For a list of antibodies, please see Table 1. FC measurement was performed on a BD LSR Fortessa II or BD Aria III, and data were analyzed with FlowJo 10 software.

Immunofluorescence of urinary bladder

Murine urinary bladders were stained for immunofluorescence as described previously.[20,37-41] Mice were euthanized 21 hours post-UPEC infection, and bladders were harvested. Bladders were fixed in PLP buffer (pH 7.4, 0.05 M phosphate buffer containing 0.1 M L-lysine, 2 mg/mL sodium periodate, and paraformaldehyde with a final wt/vol concentration of 4%) overnight at 4°C and equilibrated in 30% sucrose for 24 hours. Subsequently, bladders were embedded in Tissue-Tek OCT and cryo-conserved in *n*-hexane and dry ice at −80°C. Cryosections were rehydrated with PBT (PBS + 0.05% Triton X-100), and F_c receptors were blocked (PBT, 1% bovine serum albumin, 1 hour). Sections were stained with antibodies in blocking buffer and imaged with a Zeiss AxioObserverZ1. The cellular density and bacterial burden in UTIs were analyzed using ImageJ and R. An intensity threshold was used to generate masks for each fluorescent channel, and the binary information for cellular and nuclear signals was coregistered. Automated analysis of cell densities was performed by a Java-based algorithm. Using ImageJ, overlapping mask regions were employed to identify cells, which were marked with a point at the center of the 4′,6-diamidino-2-phenylindole (DAPI)$^+$ cell nucleus. The bladder tissue was segmented into lumen, urothelium, and connective tissue by employing the EpCAM-1 signal, and cell densities were calculated.

Neutrophil cell isolation

Neutrophils were isolated in a 2-step approach: (1) negative isolation of neutrophils via magnetic-activated cell sorting (MACS; Neutrophil Isolation Kit; Miltenyi) with CD19 MACS beads to increase the magnetic labeling of CLL B cells and (2) cell sorting via Ly6G. Sorted Ly6G$^+$ neutrophils were centrifuged, and dry pellets were shock-frozen and stored at −80°C.

Sample preparation and liquid chromatography with tandem mass spectrometry (LC-MS/MS) analysis

Cell-sorted neutrophils were lysed in 50 mM ammonium bicarbonate buffer containing 0.1% RapiGest Surfactant. The samples were reduced with 20 mM dithiothreitol for 30 min at 60°C and subsequently alkylated with 15 mM iodoacetamide for 30 minutes

Table 1. Key resource table

Reagent or resource	Source	Identifier, catalog/stock no.
Antibodies		
CD5	eBioscience	45-0051-82
CD16 human	BD Bioscience	557744
CD19	BioLegend	115539, 115507
CD45	BioLegend	103154
CD62L	BioLegend	104437
CD62L human	BD Bioscience	560440
CD66b human	Beckmann Coulter	IM0531U
Chicken anti-GFP	Aves	GFP-1020
CXCR4	BioLegend	146511
CXCR4 human	BioLegend	306506
ICAM-1	BioLegend	116105
ICAM-1 human	eBioscience	17-0549-42
Ly6G	BioLegend	127607
Reagents		
2-Iodacetamide	Merck	8.047.440.025
Ammonium hydrogen carbonate	PanReac AppliChem	A3583 0500
Bovine serum albumin	GE Healthcare	K45-001
Collagenase	Sigma-Aldrich	C2674
DAPI	Life Technologies	D1306
Dithiothreitol	PanReac AppliChem	A1101 0025
DNase I	Sigma-Aldrich	D4513-1VL
Isoflurane	Abbott	NA
LB medium	Carl Roth GmbH	X64.
L-lysine	Sigma-Aldrich	L5626
Neutrophil isolation kit	Miltenyi Biotec	130-097-658
Paraformaldehyde	Sigma-Aldrich	P6148
PBS	Life Technologies	18912-014
pHrodo Green E coli BioParticles Conjugate for Phagocytosis	Thermo Fisher Scientific	P35366
Phosphate buffer	Sigma-Aldrich	71500
[$NaH_2PO_4 + Na_2HPO_4$]	Carl Roth GmbH	P030.1
RapiGest SF surfactant	Waters	186001861
Sodium periodate ($NaIO_4$)	Carl Roth GmbH	2603.1
Sucrose	Carl Roth GmbH	9097.1
Tissue-Tek OCT	Sakura	4583
Trifluoroacetic acid	VWR	85.049.001
Triton X-100	Carl Roth GmbH	3051.4
Trypsin	Serva	37286
Experimental models: mouse strains		
C57BL/6 J	Jackson Laboratories	000664
UPEC strain 536^{gfp} (O6:K15:H31)	Engel et al[34]	doi:10.1128/IAI.00881-06

Table 1. (continued)

Reagent or resource	Source	Identifier, catalog/stock no.
Software		
Adobe Illustrator CC 2020	Adobe	RRID:SCR_010279
Fiji	ImageJ	RRID:SCR_003070
FlowJo 10	FlowJo	RRID:SCR_008520
GSEA, version 4.0.3	Broad Institute	RRID:SCR_003199
GraphPad Prism 8	GraphPad Software	RRID:SCR_002798
R Project for Statistical Computing, version 3.5.1	https://cran.r-project.org/	RRID:SCR_001905
ZEN Digital Imaging for Light Microscopy, ZEN 2012	Zeiss	RRID:SCR_013672

NA, not available.

at room temperature protected from light. Proteins were digested using 22.5 ng trypsin per sample overnight. The digestion was stopped by adding 0.5% trifluoroacetic acid, and precipitated RapiGest was removed by centrifugation. Peptides were dried in vacuo and analyzed as described before.[42] Briefly, 350 ng peptides in a volume of 15 μL 0.1% trifluoroacetic acid was subjected to an Orbitrap Elite mass spectrometer coupled to an Ultimate 3000 RSLCnano system. The peptides were preconcentrated for 7 minutes on a trap column (Acclaim PepMap 100, 300 μm × 5 mm, C18, 100 Å, flow rate 30 μL/min) and subsequently separated on an analytical column (Acclaim PepMap RSLC, 75 μm × 50 cm, nano Viper, C18, 2 μm, 100 Å) by a gradient from 5% to 40% solvent B over 98 minutes (flow rate 400 nL/min; column oven temperature 60°C). Full-scan MS spectra were acquired in the Orbitrap analyzer, and the 20 most abundant peptides were selected for MS/MS analysis (data-dependent acquisition). Tandem spectra were measured in the linear ion trap following peptide fragmentation by collision-induced dissociation.

Protein identification and data analysis

Peptides were identified using Proteome Discoverer Software (v.1.4.1.14). The mass spectra were searched against UniProtKB/Swiss-Prot database (release 2016_05, 551 193 entries) restricted to *Mus musculus* using the Mascot search engine (v.2.5). The mass tolerance was set to 5 ppm for precursor ions and 0.4 Da for fragment ions. One tryptic miscleavage was considered as well as chemical modifications of methionine (oxidation) and cysteine (propionamide). The percolator function, implemented in proteome discoverer, was used to estimate peptide confidence, and only peptides that passed a false discovery rate (FDR) <1% (FDR-adjusted $P < .01$) were considered for analysis. Ion intensity–based label-free quantification was performed using *Progenesis QI* for proteomics. To account for retention time shifts, LC-MS runs were aligned to one run automatically chosen by the software. A master list of features considering retention time and m/z was generated considering peptide ions with minimum 3 isotopic peaks and charges states +2, +3, and +4. The peptide identifications (peptides spectrum matches) from Proteome Discoverer were imported into the software and matched to the respective features. The protein abundances were calculated considering the normalized ion intensities of all nonconflicting peptides of a protein. Normalized protein intensities were further analyzed using R.

Pathway enrichment analysis and STRING

Gene set enrichment analysis (GSEA) was performed using the molecular signature database (MSigDB v7.1). STRING was used to analyze protein-protein interactions of the significant proteins (FDR-corrected $P < .01$) of blood neutrophils in CLL vs non-CLL.

Machine learning

The intensity of data were normalized by dividing each data point by the 75th percentile of the corresponding sample. Features were selected based on P values computed with the χ^2 test and corrected for multiple testing via the Benjamini-Hochberg method post hoc.[43-45] Only features with an FDR-adjusted $P \leq .01$ were retained. With the remaining features (proteins), a RFC was trained.[44,46] Our RFC was trained with 300 trees in a 1-vs-1 manner; thus, for each class comparison, 1 RFC was trained. The performance of the RFC was evaluated in a stratified fivefold cross-validation.

Statistical analysis

Results are presented as mean $\pm$ standard error of the mean (SEM). Normality was tested with the D'Agostino-Pearson omnibus test. Two groups were compared with the Mann-Whitney test. Kruskal-Wallis with Dunn's post hoc tests were used for comparison of >2 groups. Two-way analysis of variance with post hoc Bonferroni correction were used for longitudinal experiments. Linear regression was used to determine the R^2. Volcano plots were generated using paired and unpaired Student t tests. Resulting P values were adjusted to control the FDR according to Benjamini-Hochberg. Significance and normal distribution were calculated using R and Graph Pad Prism 8.

Results

Increased susceptibility to bacterial UTI in CLL

Patients with CLL suffer from recurrent and often severe bacterial infections.[3-13] In a CLL in vivo model, we observed a massive expansion of CLL (CD5^{+}CD19^{+}) cells in the BM and blood (supplemental Figure 1A-D). As patients with CLL are predisposed to bacterial infections, the susceptibility of CLL-bearing mice to UTI was determined.[21] After inoculation of UPEC into the urinary bladder, we detected large bacterial communities in CLL-bearing mice (Figure 1A), and the overall bacterial burden in the lumen ($P < .0001$) and urothelium ($P < .01$) was significantly increased in CLL-bearing mice compared with nonleukemic controls (Figure 1B). These data demonstrate that CLL predisposes to aggravated bacterial infections of the urinary bladder.

Proteomics reveals impact of CLL on neutrophil phenotype

Neutrophils are critical leukocytes that facilitate the immediate defense response in bacterial infections.[21] These cells develop in the BM, are released into the bloodstream, and migrate into the urinary bladder upon infection.[47] Since malignant B cells heavily accumulate in the BM and blood in CLL, we hypothesized that these cells shape neutrophil phenotype and functionality at these sites, subsequently predisposing to bacterial infections. Hence, we performed a proteome analysis by using LC electrospray ionization coupled to MS/MS on sorted neutrophils. To assess the impact of CLL on the neutrophil proteome, a RFC was used to generate

a receiver operating characteristic curve. Using this RFC, we found that the proteomic signature of neutrophils showed a perfect classification of the datasets from non-CLL vs CLL-bearing mice (Figure 2A-B). Next, we visualized the proteomic differences of neutrophils of non-CLL and CLL-bearing mice using the fold change and FDR-adjusted P value in a volcano plot representation (Figure 2C-D, supplemental Tables 2 and 3). Such analysis identified 82 proteins in the BM and 144 in the blood with significant alterations due to differences in the protein abundancy (FDR-adjusted $P < .01$; Figure 2E-F; supplemental Tables 2 and 3). Using unsupervised multivariate analysis by a principal-component analysis, we observed that the CLL environment has a more significant impact on blood over BM neutrophils, as indicated by an increased distance of the blood clusters in non-CLL vs CLL in the first dimension (Figure 2G).

STRING and GSEA identify aberrations in neutrophil functionality in CLL and provide targets for therapeutic interventions

Next, we further investigated the interactions of the 144 differentially expressed proteins by STRING.[48] Such analysis identified clusters for IFN signaling, ribosomes, granules, and migration (Figure 3A; supplemental Table 4). Further analysis of the proteins from the individual clusters indicated that the IFN-response and ribosomal proteins were upregulated in the CLL conditions, whereas components of granules and neutrophil migration were mostly downregulated in CLL (Figure 3B). In particular, IFN-induced protein with tetratricopeptide repeats 3 and IFN-stimulated gene 15 (ISG15) were significantly enriched in the IFN cluster, whereas thrombospondin, L-selectin (CD62L/LYAM1), elastase, lysozyme, and myeloperoxidase (MPO; PERM) were clearly downregulated in the granules and migration cluster (Figure 3B). Subsequently, we performed a GSEA of the neutrophil proteome to identify pathways with classes of proteins that are over- or underrepresented in neutrophils of CLL-bearing mice. Such analyses revealed 66 pathways with a positive normalized enrichment score (NES), indicating an upregulation in CLL (supplemental Table 5). In addition, 26 pathways were found with a negative NES, indicating that these protein classes were downregulated in CLL (supplemental Table 6). Visualization of the 10 pathways with the largest NES difference indicated enriched protein classes for IFN-response, ribosomes, and metabolism (Figure 3C; supplemental Table 5), while the proteins classes of secretory granules and neutrophil migration were lower expressed, as shown by a negative NES (Figure 3D; supplemental Table 6). Thus, blood neutrophils in CLL-bearing mice reveal a distinct proteomic signature suggesting an aberrant composition of neutrophil granular content and altered migratory capacities.

To widen our understanding of the IFN-related alterations in the neutrophil proteome, we focused on the most enriched pathways: "*IFNγ* response" and "*IFNα* response" (supplemental Tables 7 and 8). Based on a total of 32 differentially expressed proteins in both pathways (Figure 4A), we identified 17 common proteins that are ordered according to their rank metric score in the heatmap (Figure 4B). Furthermore, a machine learning algorithm identified IFN-dependent molecules that mostly contributed to the separation of the proteome datasets in CLL. Here, an RFC was employed to ensure interpretability and reproducibility. The best features of the neutrophil proteome were obtained based on their Gini decrease,
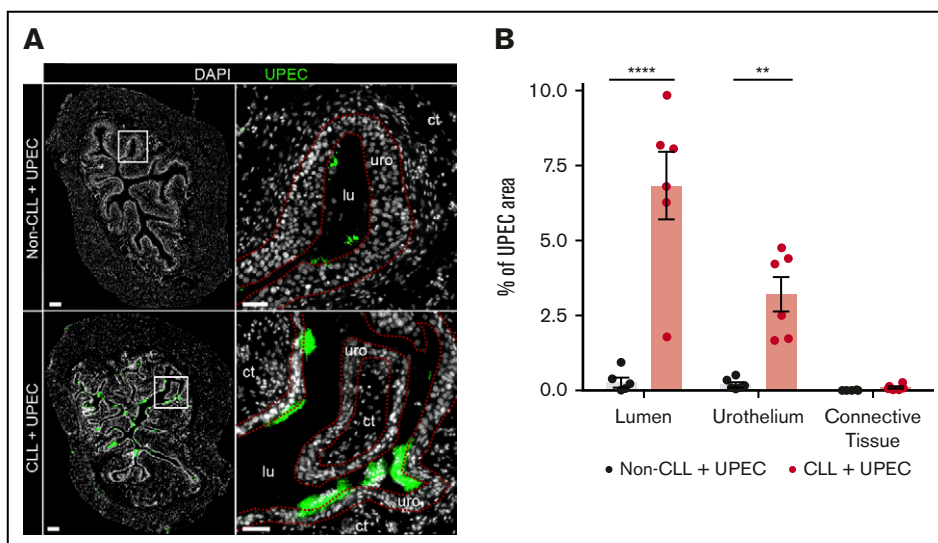
Figure 1. Increased acute infection of the urinary bladder in CLL. (A) Urinary bladders of CLL mice with a tumor burden of >20% and non-CLL mice were infected with UPEC[GFP], and the bacterial burden was determined on day 1 postinfection by fluorescence microscopy. The dashed lines indicate the border of the urothelium to the lumen and connective tissue. DAPI is shown in white and UPEC[GFP] in green. Scale bars, 200 μm (left panel) and 50 μm (right panel). (B) Quantification of the microscopic images shown in panel A. The bacterial burden was calculated as UPEC-positive area in the indicated bladder tissues (lumen, urothelium, and connective tissue) in UPEC-infected non-CLL and CLL-bearing mice. **$P < .01$, ****$P < .0001$ (n = 6). Data represent mean ± SEM. ct, connective tissue; lu, lumen; uro, urothelium.

which itself is a measure for the goodness of feature. Such analysis identified ISG15, immunity-related GTPase family M protein 1, and IFN-induced protein 35 (Figure 4C), corroborating our previous STRING analysis and GSEA.

Altered composition of neutrophil granule proteins and dysfunctional acidification of granules in neutrophils in CLL

Next, we extended the characterization of neutrophils in regard to their functionality by performing GSEA of the most downregulated proteins of the pathways "secretory vesicle" and "secretory granules" (Figure 5A; supplemental Figures 9 and 10). The analysis revealed proteins that are essential for neutrophil phagocytosis and degradation of bacterial components through granular compartments, such as lysozyme, elastase, and myeloperoxidase (PERM) (Figure 5B). Notably, proteomic data also unveiled an increased abundance of ceruloplasmin, an endogenous MPO inhibitor, in blood neutrophils of CLL-bearing mice (Figure 5C). In order to study whether the altered expression of the proteins from the GSEA affects the effector functions of neutrophils in CLL, the expression of MPO and acidification of granules after phagocytosis were tested in blood neutrophils ex vivo through the ingestion of pH-sensitive fluorochrome-tagged *E coli*. FC demonstrates that neutrophils expressed significantly less MPO ($P < .01$), suggesting impeded peroxidase activity of neutrophils in CLL (Figure 5D). In line with this finding, we also observed a significantly reduced ($P < .01$) acidification in neutrophils in CLL after phagocytosis of pH-sensitive fluorochrome-tagged *E coli* (Figure 5E). Collectively, these data show severe abnormalities of neutrophil effector functions in CLL-bearing mice.

Compromised neutrophil migration in CLL

STRING suggested reduced migration of neutrophils, and GSEA identified downregulation of the pathways "ECM," "focal adhesion,"

"cell-cell adhesion," "leukocyte cell-cell adhesion," and "granulocyte migration" (Figure 3D; supplemental Figures 11-15). In order to identify the proteins that contributed to the high significance level in the GSEA and to the negative NES, we extracted the proteins from the GSEA plots (Figure 6A). We observed reduced expression of CD62L (LYAM1) in CLL-bearing mice, implying that this protein might be critically involved in neutrophil migration to infected organs (Figure 6B). Notably, hemopexin, an inhibitor of neutrophil migration, was expressed at increased levels in CLL (supplemental Figures 2 and 3). Furthermore, MMP9, a critical enzyme for neutrophil migration,[21] was decreased in CLL (Figure 6B). To evaluate whether these changes alter neutrophil migration in vivo, we infected mice with UPEC, and the number of recruited neutrophils was quantified by fluorescence microscopy. We observed a significant impairment of neutrophil migration into the infected urinary bladder ($P < .01$) in relation to the aggravated infection in CLL-bearing mice (Figure 6C). Collectively, these data demonstrate decreased migratory capacity of neutrophils in severe infections in CLL-bearing mice.

Aberrant expression of surface molecules important for neutrophil migration

As a result of the proteomic findings, we validated the expression of CD62L, which was the most differentially abundant surface molecule. We observed significant downregulation of CD62L by FC, suggesting a more mature phenotype of neutrophils in CLL-bearing mice. As CXCR4 is highly relevant for the egress of mature neutrophils from the BM, we also determined the expression of CXCR4.[49] We found that neutrophils in CLL-bearing mice expressed significantly less CXCR4 ($P < .05$) (Figure 7A-C; supplemental Figure 16), corroborating the hypothesis of a more mature phenotype of neutrophils in CLL-bearing mice. Correlation analyses illustrated that these alterations in the expression of the surface molecules were associated with CLL disease progression
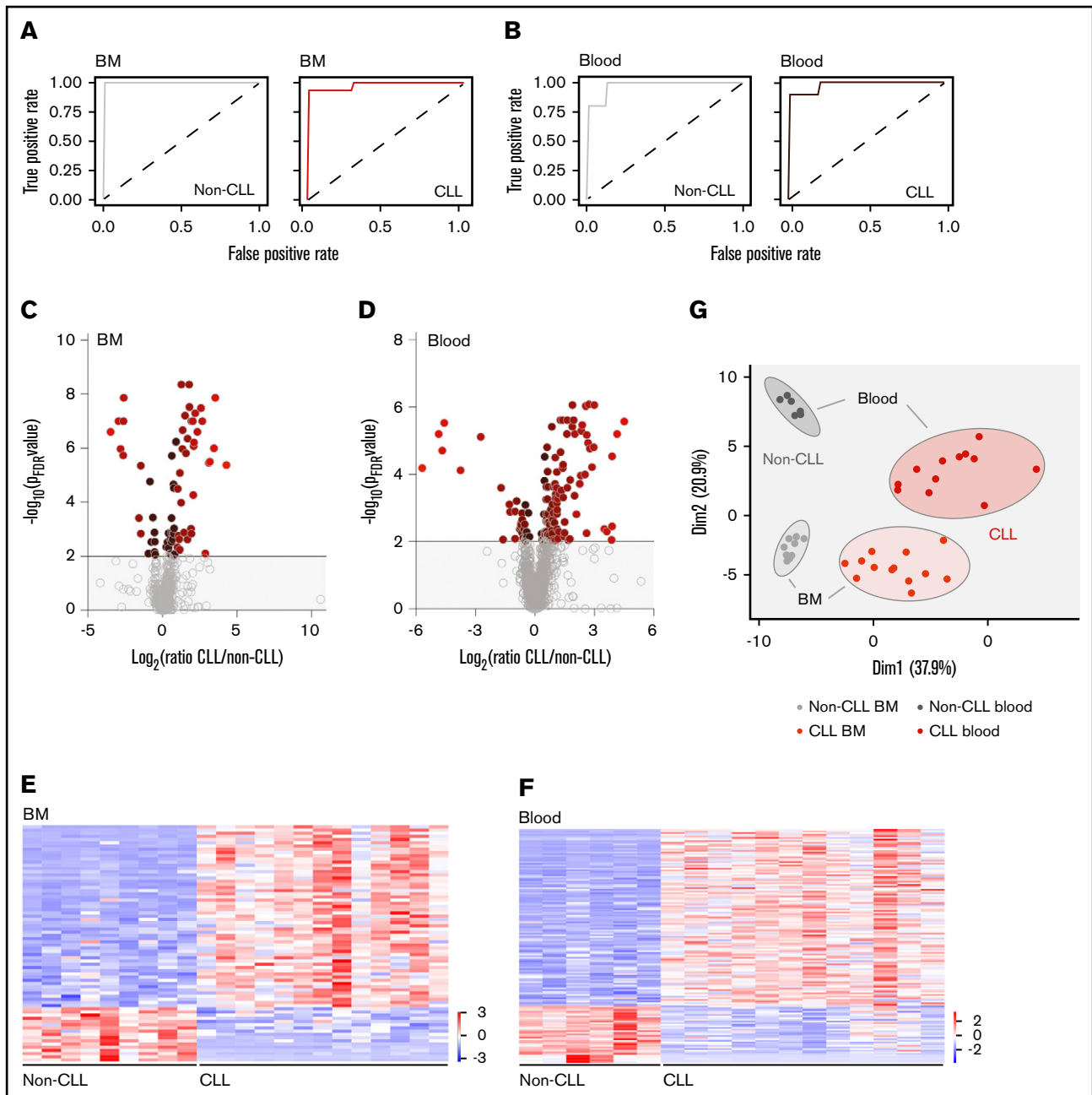
Figure 2. Aberrant proteome of neutrophils in CLL. Neutrophils from the BM and blood of non-CLL and CLL-bearing mice were isolated by cell sorting, and the proteome was analyzed by LC-MS/MS. (A-B) Receiver operating characteristic curves based on proteome of BM (A) and blood (B) neutrophils indicate alterations in non-CLL and CLL conditions. (C-D) Volcano plots illustrating fold change (log$_2$, x-axis) vs FDR-adjusted P value ($-$log$_{10}$ [FDR], y-axis) of the neutrophil proteome in the BM (C) and blood (D). The gray lines indicate the proteins that have passed a significance value of <.01 ($-$log$_{10}$ [FDR] >2). (E-F) Heatmaps of significant proteins from the volcano plots in panels C and D with an FDR-adjusted P < .01. Expression values of all proteins are shown in supplemental Tables 2 and 3. (G) Principal-component analysis of the significant proteins (FDR-adjusted P < .01) in the BM and blood indicate alteration of the neutrophil proteome in the blood of CLL-bearing mice. BM: non-CLL, n = 9; CLL, n = 13; blood: non-CLL, n = 6; CLL n = 12.

(Figure 7D-E). Subsequently, the downregulation of both molecules was also assessed in a translational approach in 14 patients with CLL. In line with our in vivo data, we also found a significant decreased expression of CD62L (P = .0409) and a trend for reduced CXCR4 expression on neutrophils in the CLL condition (Figure 7F; supplemental Figure 17). Linear regression analysis of

the expression of these surface molecules suggested a correlation with disease progression (Figure 7G-H). Hence, the aberrant expression of CD62L and CXCR4 may serve as a potential signature on neutrophils that contributes to an impaired migration into infected organs. In our CLL cohort, we also observed frequent bacterial infections in the lung (supplemental Table 18). The course
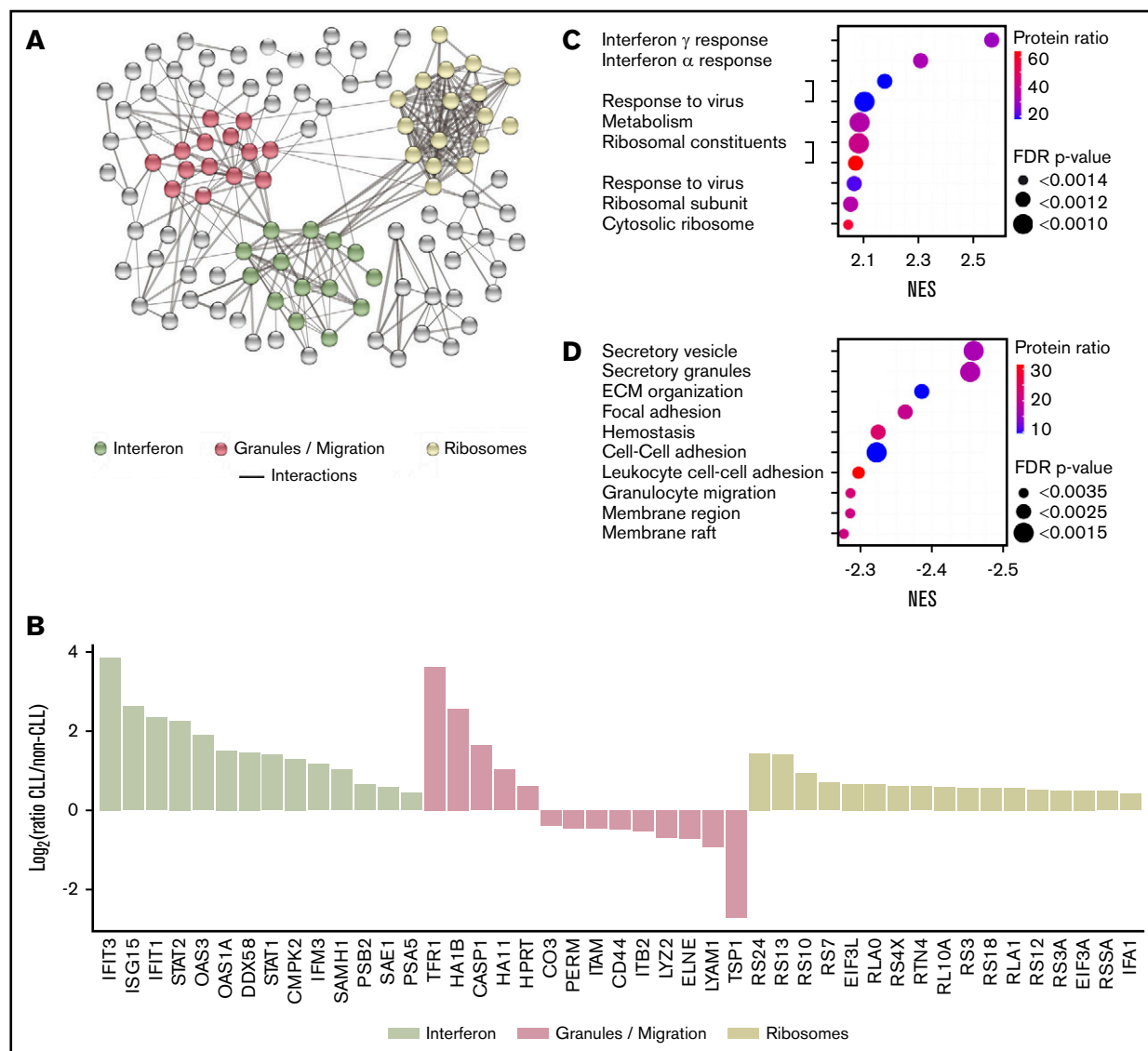
Figure 3. Increased IFN signaling and decreased protein expression critical for secretory granule and migration in blood neutrophils from CLL-bearing mice. (A) STRING analysis of the significant proteins ($P < .01$) of blood neutrophils from CLL-bearing mice. K-means clustering indicated enriched protein-protein interactions in the protein network. See supplemental Table 4 for a more detailed table. (B) Dot plot illustrating fold changes ($\log_2$ of CLL vs non-CLL) of individual proteins of clusters indicated in panel A. (C-D) GSEA of the proteome of blood neutrophils in CLL vs non-CLL conditions. NESs were displayed in different sizes to reveal the FDR-adjusted P value and in different colors to indicate the protein ratio within the indicated pathway. See supplemental Tables 5 and 6 for more detailed tables. Non-CLL, n = 6; CLL, n = 12.

of these respiratory infections is often severe in patients with CLL and a frequent cause of death.[3-7] Hence, we retrospectively analyzed the incidence of respiratory infections in these patients and found that the incidence of respiratory infections significantly increased ($P = .0341$) with the CLL burden (Figure 7I), strengthening our hypothesis that the observed changes in the neutrophil signature may be one important aspect leading to not only increased UTIs but also respiratory infections in patients with CLL.

Discussion

Frequent and severe bacterial infections account for more than two-thirds of all infections in patients with CLL.[3-7,10-13] These complications often prevent patients with CLL from undergoing

antileukemic therapies, imposing an economic and individual burden.[10] Targeting neutrophils to restore the antibacterial response via their essential functions, such as migration, phagocytosis, and degranulation, should become the focus during the clinical development of treatment options for patients with CLL. On the one hand, the increased risk of infections can be reduced to avoid secondary morbidities, and on the other hand, anti-CLL treatment regimens will not have to be interrupted.

In this study, we show an increased susceptibility of CLL-bearing mice to UTIs. Given that neutrophils are the most critical immune cell population during UTI, we generated a proteomic fingerprint and performed phenotypic and functional analyses to provide novel insights into the potential immunosuppression of neutrophils in CLL.
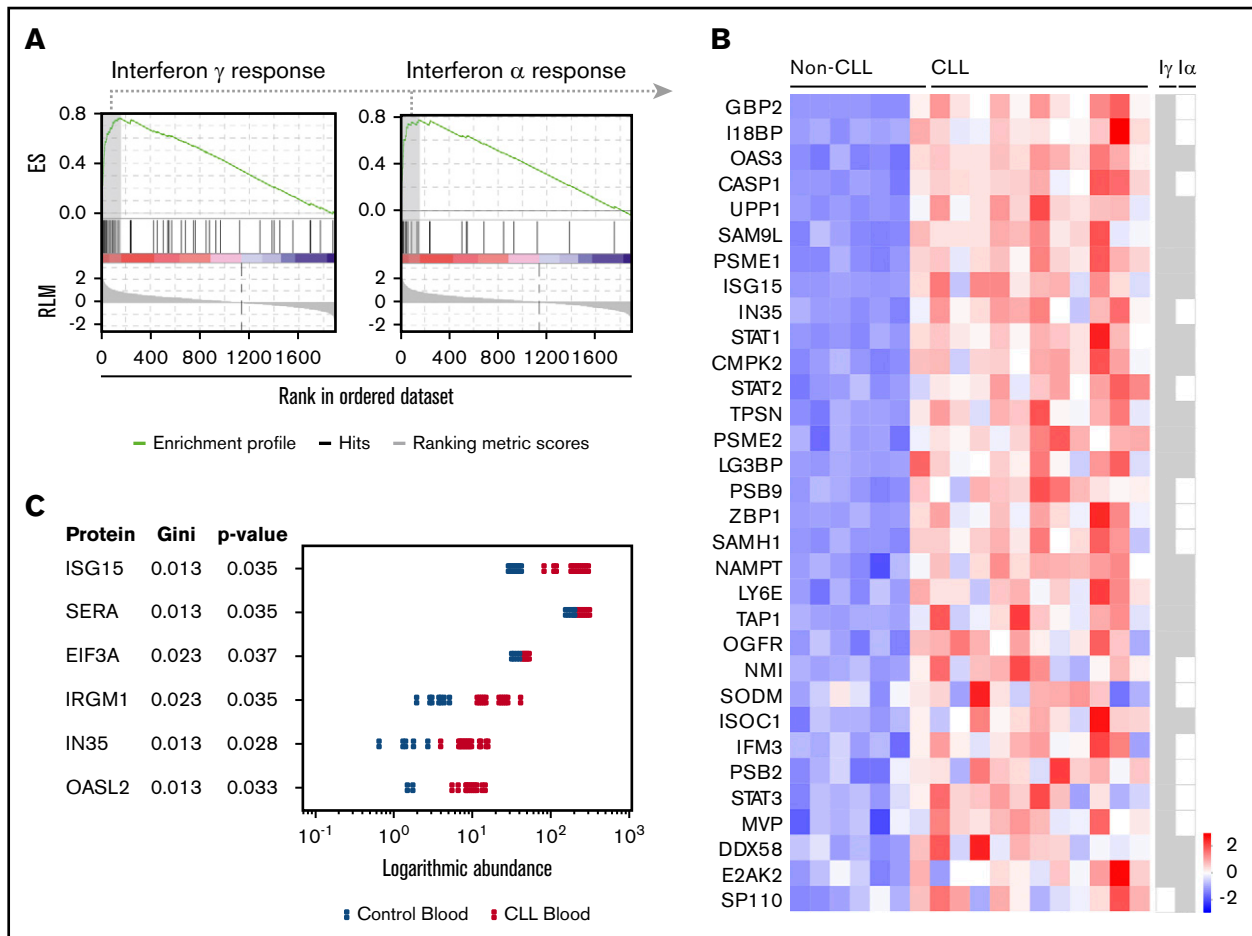
Figure 4. Identification of proteins involved in increased IFN signaling in blood neutrophils during CLL. (A) GSEA of the proteome of blood neutrophils indicated a significant enrichment of *IFN*γ and *IFN*α response. The positive enrichment score (ES) indicates the contribution of those proteins that are overexpressed in blood neutrophils in CLL-bearing mice. Detailed expression values are shown in supplemental Tables 7 and 8. (B) Analysis of the enrichment score indicated 31 significantly enriched proteins of the pathway "*IFN*γ response" (Iγ) and 18 proteins of the pathway "*IFN*α response" (Iα). The heatmap indicates the expression intensities of proteins of both pathways, "*IFN*γ and -α response," in blood neutrophils of CLL-bearing mice. (C) A machine learning algorithm of the proteome of blood neutrophils in CLL indicates best features in according to logarithmic abundances. A RFC was used to calculate the Gini decrease. RLM, ranked list metric. Non-CLL, n = 6; CLL, n = 12.

We describe that important functions of neutrophils, such as MPO production, intracellular granular content, acidification of the phagolysosome after phagocytosis of bacteria, and migration of neutrophils into the infected urinary bladder were suppressed in CLL-bearing mice. Thus, a molecular signature of neutrophils was generated that might be associated with severe bacterial infections in CLL.

Phagocytosis and degradation of UPEC critically reduce the bacterial burden in the urinary tract.[20,21] Previously, functional defects regarding antibacterial responses were observed in patients with CLL.[27] Using enrichment analysis of the neutrophil proteome, we observed impaired expression of neutrophil granule proteins and upregulation of inhibitors, such as ceruloplasmin.[50] Moreover, functional assays indicated impeded acidification of the phagolysosome after phagocytosis of bacteria. Proteome analysis of sorted neutrophils revealed that key molecules regulating the migration, such as MMP9, were downregulated in CLL.[21] Accordingly, the invasion of neutrophils from the blood into the infected urinary bladder was less efficient in CLL-bearing mice with severe

UTI. These data indicate that important antimicrobial core competencies of neutrophils are impaired in CLL. It is also conceivable that other functions of neutrophils are impacted, such as the formation of neutrophil extracellular traps, and production of inflammatory cytokines that subsequently would regulate the antimicrobial response, are equally repressed in the CLL condition.

Neutrophil migration from the blood into the infected organs also involves adhesion molecules, chemokines, integrins, and selectins.[51] We observed that the reduced migratory capacity was associated with aberrant expression of CD62L and CXCR4, indicating a more mature and activated phenotype of blood neutrophils in CLL. Previously, altered expression of these molecules was described for aged neutrophils also in other disease contexts.[52-54] Interestingly, a similar phenotype with low CD62L and CXCR4 expression on neutrophils has been observed as tumor-promoting neutrophils in a solid cancer model, which might account for the impairment of neutrophil effector functions and subsequent risk of bacterial infections in CLL.[55] Declining frequencies of CXCR4-expressing neutrophils may have several causes, including an
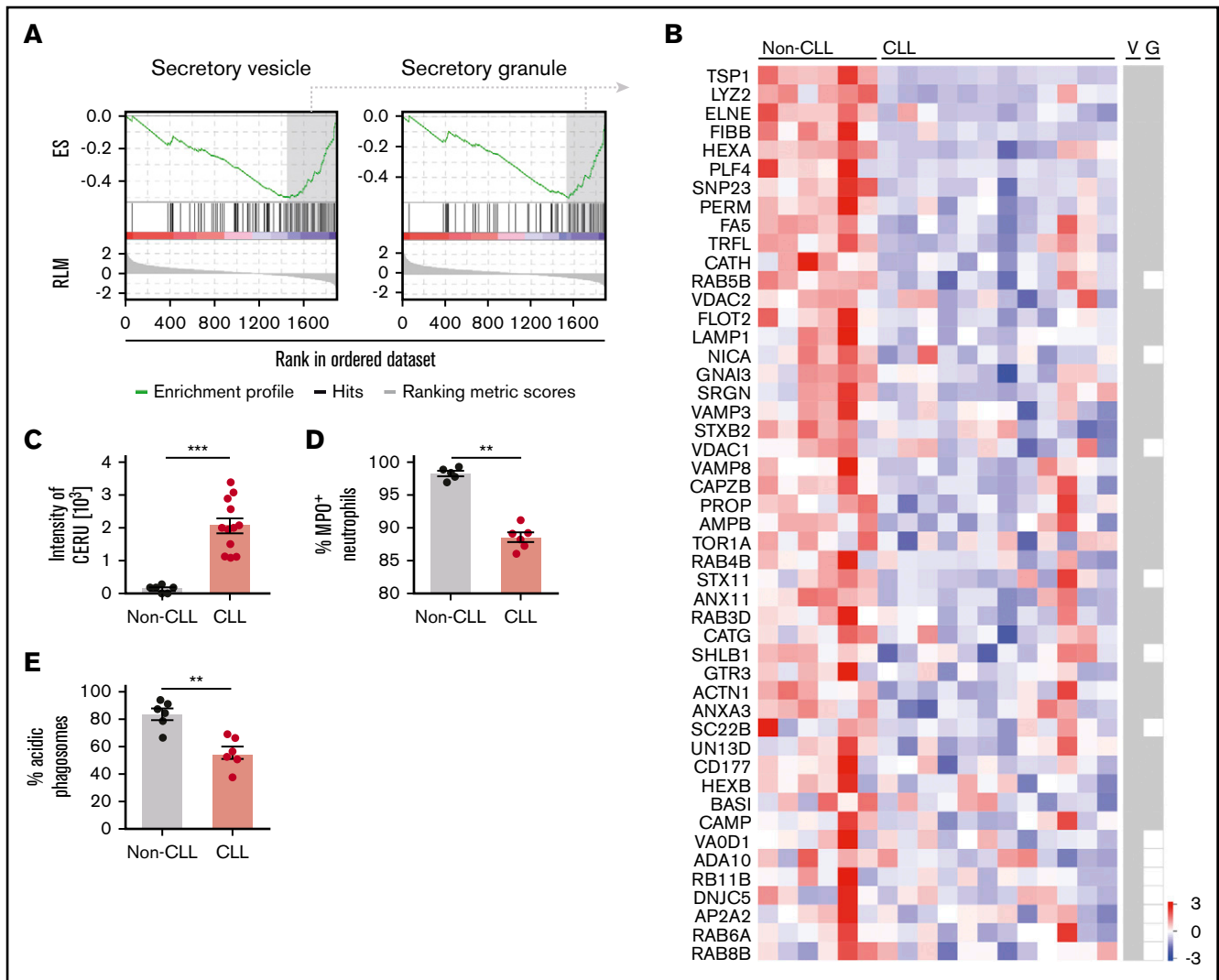
     blood advances

Figure 5. Neutrophils in CLL show aberrant function. (A) GSEA of the proteome of blood neutrophils indicated pathways with reduced expression of proteins of the secretory vesicles and granules. Detailed expression values are shown in supplemental Tables 9 and 10. (B) Analysis of the enrichment score indicated 48 significantly downregulated proteins of the pathway "secretory vesicle" and 35 proteins of the pathway "secretory granule". The heatmap visualizes the expression intensities of proteins of both pathways (secretory vesicle and secretory granule) in blood neutrophils of CLL-bearing mice. (C) Expression intensity of ceruloplasmin on blood neutrophils determined by LC-MS/MS. (D) MPO expression in neutrophils from non-CLL and CLL-bearing mice were analyzed by FC. (E) Neutrophils from non-CLL and CLL-bearing mice were incubated with pH-sensitive *E coli* and then analyzed by FC to determine the level of the acidification of phagolysosomes postphagocytosis of the bacteria. **$P < .01$, ***$P < .001$. Data represent mean ± SEM. (A-C) Non-CLL, n = 6; CLL, n = 12. (D) Non-CLL, n = 5; CLL, n = 6. (E) Non-CLL, n = 6; CLL, n = 6. CERU, ceruloplasmin; G, secretory granule pathway; V, secretory vesicle pathway.

altered release of neutrophils from the BM[49] or spleen[56] or a more rapid maturation in the circulation. We also observed decreased expression of GRB2, which is critical for proliferation and differentiation of myeloid progenitors into neutrophils.[57] This finding supports the former suggestion of an altered release of neutrophil progenitors from the BM into the circulation.[57] By extending this finding into a clinical context, CXCR4 could be used as a biomarker, while GRB2 might serve as a putative target to enhance neutrophil proliferation and differentiation in patients with CLL. This could potentially strengthen essential neutrophil functions, such as phagocytosis and degranulation to fight off infections. Furthermore, CD62L is being shed upon stimulation and is thus widely described as a functional marker to determine

the activation status of neutrophils[58,59]; also, in CLL, reduced expression of CD62L was recently described for neutrophils from clinical samples.[28,29] In these studies, neutrophil subsets were not correlated to CLL load in the circulation, but compared with healthy age-matched samples, which does not stratify neutrophil alterations during CLL disease progression. We demonstrate a gradual loss of CD62L in different CLL stages and, interestingly, CD62L was also shown to be decreased by hemopexin in sepsis,[60] a molecule highly abundant in our proteome dataset in CLL-bearing mice.

Enrichment analysis indicated increased expression of proteins involved in IFN signaling. After ligand binding to the IFN receptors, JAK is activated via phosphorylation, subsequently culminating in STAT1 and STAT2 pathway activation in the same manner.[61] In
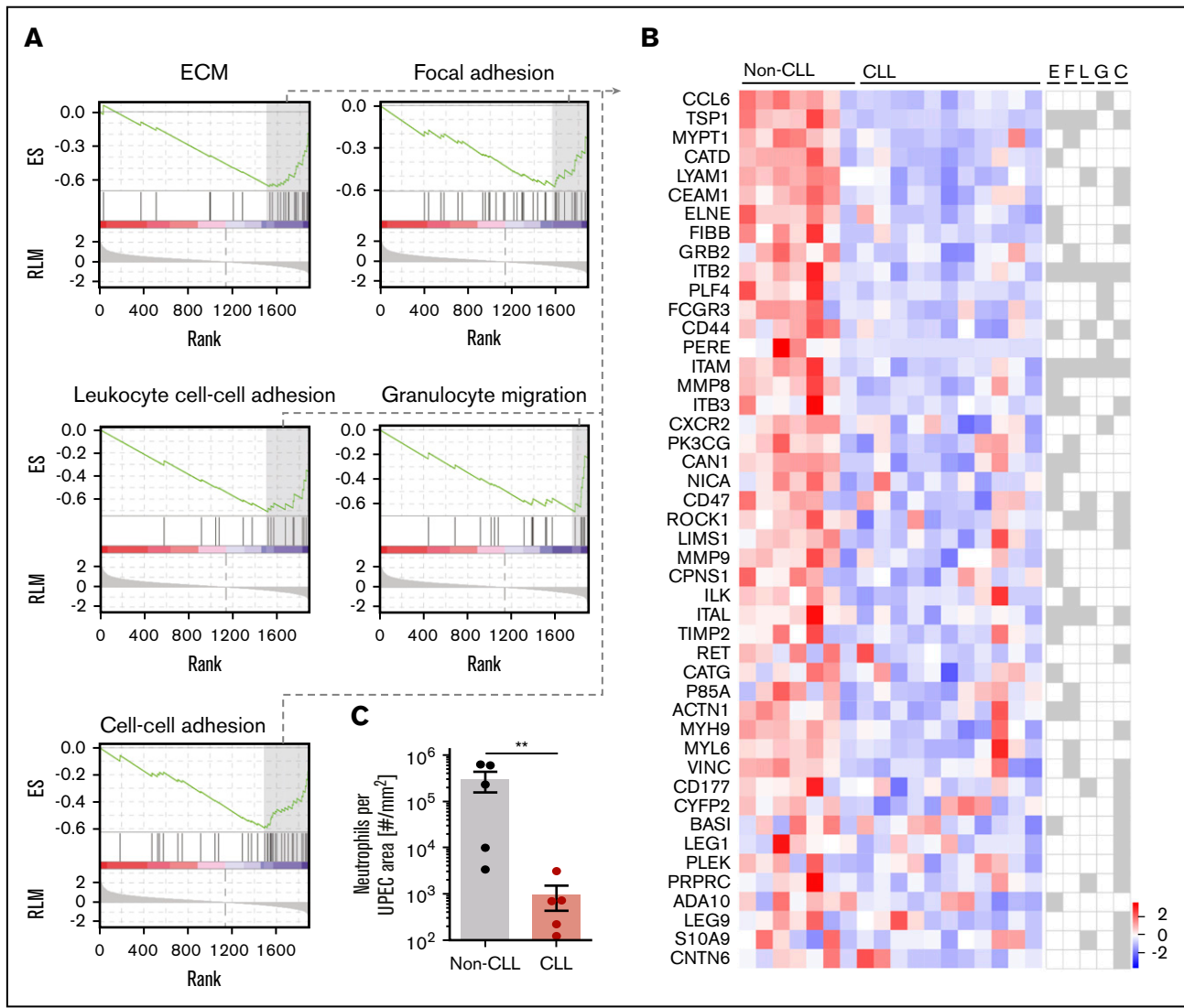
Figure 6. Neutrophils in CLL show impaired migration after bacterial infection of the urinary bladder. (A) GSEA of the proteome of blood neutrophils indicated migratory pathways to be particularly enriched with reduced expression of proteins involved in the migration of neutrophils. Detailed expression values are shown in supplemental Tables 11-15. (B) The heatmap indicates the expression intensities of proteins of the pathways extracellular matrix (ECM), focal adhesion, cell-cell adhesion, leukocyte cell-cell adhesion, and granulocyte migration in blood neutrophils in CLL-bearing mice. (C) Mice were infected with UPEC^{GFP} and the number of neutrophils per UPEC area [#/mm^2] in relation to the bacterial burden were calculated. **P < .01. Data are mean ± SEM. (A-B) Non-CLL, n = 6; CLL, n = 12. (C) Non-CLL, n = 6; CLL, n = 6. C, cell-cell adhesion; E, ECM pathway; F, focal adhesion pathway; G, granulocyte migration pathway; L, leukocyte cell-cell adhesion pathway.

particular, STAT1 activation leads to downstream activation of immunity-related GTPase family M protein 1,[62-64] which has been shown to inhibit TLR4 signaling[65] and was significantly upregulated in our proteome dataset in CLL. Moreover, aberrant IFN signaling has been associated with aggressive CLL, and the duration of IFN-mediated STAT phosphorylation was prolonged in CLL with high-risk features.[66] Our proteome data indicate increased IFN signaling in neutrophils, which may impede pattern recognition–induced responses in neutrophils, subsequently leading to severe bacterial infections in CLL.[65] We observed reduced acidification of the phagolysosome after phagocytosis of bacteria, suggesting impeded recognition of the pathogen. Interestingly, we identified ISG15 as a critical IFN-dependent molecule, which was highly upregulated in CLL and included in both pathway analysis and RFC-

based analysis. Previously, ISG15 has been observed in various cancer tissues[67,68] and is associated with local recurrence and short overall and disease-free survival.[69] Moreover, ISG15-dependent production of IFN-γ has recently been shown to depend on LFA-1,[70] and both subunits of LFA-1, ITAL and ITB2, displayed reduced expression in CLL-bearing mice. Therefore, ISG15 might play a tumor-supporting role, and our proteomic data suggest that increased ISG15 expression in neutrophils affects their function and migration. Interestingly, persistent JAK/STAT signaling was found in patients with CLL,[71] and treatment with ruxolitinib, a drug that blocks IFN signaling through JAK/STAT, reduced disease-related symptoms.[72] We hypothesize that not only these disease-related symptoms but also the molecular and functional changes in the neutrophil population are mediated through aberrant IFN
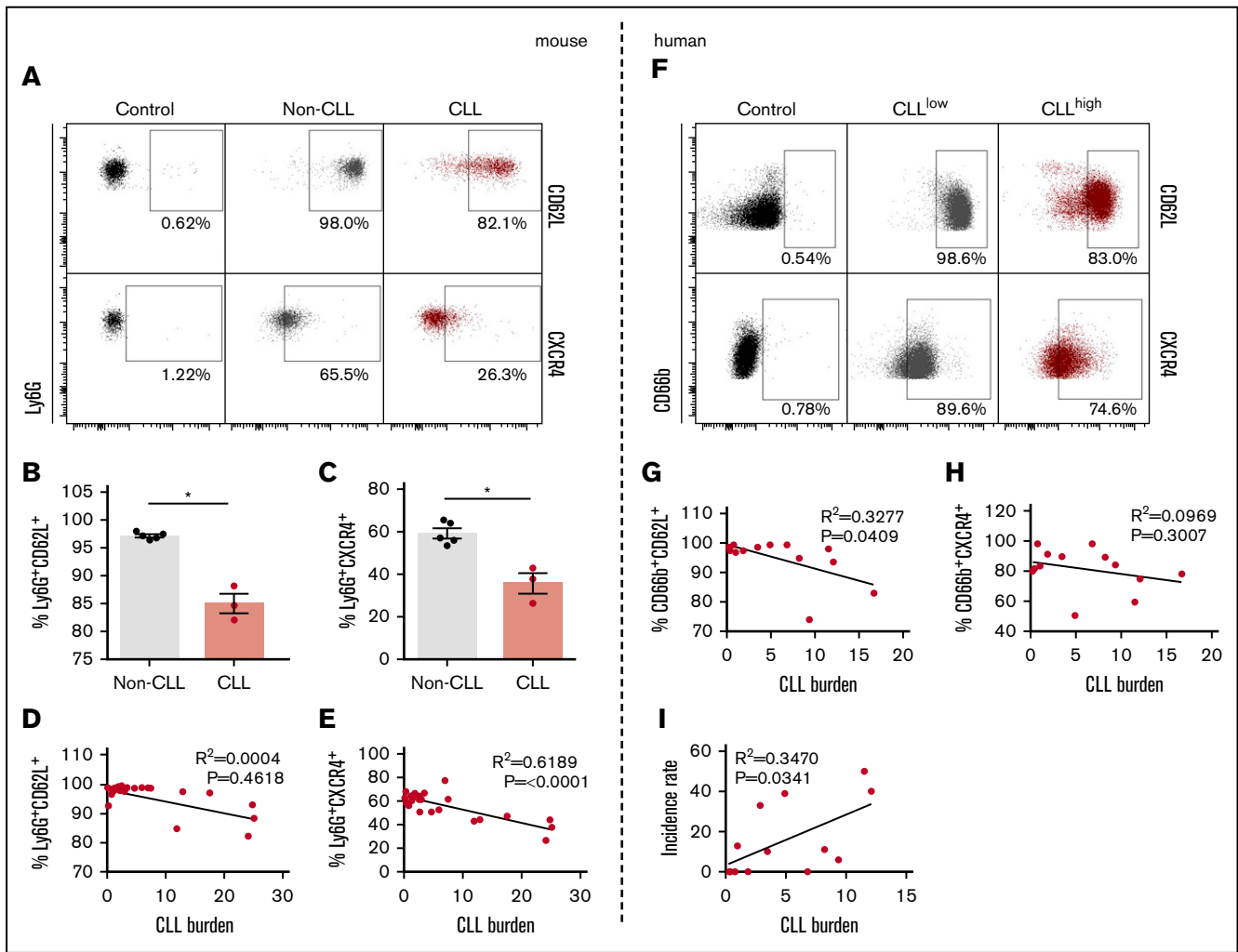
Figure 7. A distinct phenotype of blood neutrophils in CLL indicates aberrant migration during UTI. (A) Mice were induced with CLL, and the expression of CD62L and CXCR4 was determined on neutrophils by FC (gating shown in supplemental Figure 17). Dot plots indicate phenotypic alterations in protein surface expression on blood neutrophils of non-CLL (gray) and CLL-bearing mice (red). Control stainings are indicated as fluorescence minus one (FMO; black). (B-C) Mice were euthanized on day 42 post-CLL induction with a tumor burden (% CD5$^+$ CD19$^+$ in whole blood) >20%. The frequency of neutrophils for CD62L (B) and CXCR4 (C) was determined by FC. (D-E) Linear regression analysis of the indicated surface molecules on murine blood neutrophils. The CLL burden (% CD5$^+$ CD19$^+$ in whole blood) and frequencies of neutrophil subsets positive for CD62L (D) and CXCR4 (E) were determined by FC. (F) The expression of the surface molecules CD62L and CXCR4 was determined on blood neutrophils from patients with CLL (gating shown in supplemental Figure 17). Dot plots illustrate the phenotypic alterations in protein expression in patients with low CLL load (patient 2 with 34 830 lymphocytes per μL blood, gray) vs high CLL load (patient 5 with 166 939 lymphocytes per μL blood, red) analyzed by FC. Isotype control staining is also shown (black). (G-H) Linear regression analysis of CD62L (G) and CXCR4 (H) on blood neutrophils from patients with CLL (CLL burden = number of lymphocytes [×10^4]/μL blood). (I) Incidence rate of respiratory infections (percentage of infections per year of monitored period) in correlation to CLL burden (number of lymphocytes [×10^4]/μL blood) (detailed information of patient history is shown in supplemental Table 18). *$P < .05$. Data represent mean ± SEM. (A) Non-CLL, n = 5; CLL, n = 3. (F) Patients with CLL, n = 14. (A-E) Pregated on Ly6G$^+$ neutrophils (shown in supplemental Figure 16). (F-H) Pregated on CD45$^{dim/high}$ and CD16$^{-/+}$, CD45^{high} CD16$^-$ eosinophils were excluded (shown in supplemental Figure 17).

signaling. Targeting the IFN-signaling pathway in neutrophils may not only be beneficial for the disease-related symptoms but also reduce the susceptibility to infections.

In summary, molecular profiling of neutrophils in CLL reveals phenotypical alterations and functional defects that are associated with increased bacterial UTIs. We observed a potential role of IFN signaling for the suppression of neutrophils in CLL and identified altered expression of important surface molecules for neutrophil migration, such as CD62L and CXCR4. Our study also provides

a molecular signature of neutrophils in CLL with a broad range of proteins with biomarker or therapeutic potential, such as IFN-induced protein with tetratricopeptide repeats, ISG15, ceruloplasmin, hemopexin, and GRB2. Further studies are required to assess the role of these proteins for neutrophil suppression in CLL and greater susceptibilities to severe and frequent infections.

Our data may also be of importance for the defense against pathogens in other organs, such as the lung, which cause serious and life-threatening complications in patients with CLL.[3-7] Indeed,

we observed frequent lung infections in our patients with CLL, and retrospective analysis of the incidence of respiratory infections indicated that our patients with CLL suffered from multiple respiratory infections, which correlated with the CLL burden. It can therefore be concluded that the molecular signature and functional changes in the neutrophil population described by us may lead to the increased incidence of bacterial infections in patients with CLL.

Authorship

Contribution: N.S., J.B., S.T., K.Z., E.d.D.P., and J.K.L. contributed to investigation; N.S., J.B., C.S., M.K., T.B., A.P., R.H., S.R., B.S., and D.R.E. performed mass spectrometry visualization and computational analysis; N.S., J.B., P.J., K.B., and S.B. contributed to FC of human blood neutrophils; M.S., S.B., and H.C.R. provided critical reagents; N.S., J.B., H.C.R., and D.R.E. wrote the manuscript; D.R.E. provided supervision; and all authors read and commented on the paper.

Conflict-of-interest disclosure: H.C.R. is a cofounder of CDL therapeutics and received consulting fees from AbbVie, Vertex, Merck, and AstraZeneca and contract research funding from Gilead. The remaining authors declare no competing financial interests.

ORCID profiles: N.S., 0000-0003-2161-6827; J.B., 0000-0002-4418-6092; S.T., 0000-0001-5320-3889; K.Z., 0000-0003-1005-2368; M.K., 0000-0003-0733-9210; C.S., 0000-0002-9993-158X; E.d.D.P., 0000-0003-3660-8061; A.P., 0000-0002-0114-1812; S.R., 0000-0002-8536-6065; P.J., 0000-0002-3265-8689; T.B., 0000-0002-1194-6614; D.R.E., 0000-0001-7301-353X.

Correspondence: Daniel Robert Engel, Institute of Experimental Immunology and Imaging, University Hospital Essen, Department of Immunodynamics, Medical Research Center, Hufelandstr 55, 45147 Essen, Germany; e-mail: danielrobert.engel@uk-essen.de.

References

1. Miranda-Filho A, Piñeros M, Ferlay J, Soerjomataram I, Monnereau A, Bray F. Epidemiological patterns of leukaemia in 184 countries: a population-based study. *Lancet Haematol*. 2018;5(1):e14-e24.

2. Kipps TJ, Stevenson FK, Wu CJ, et al. Chronic lymphocytic leukaemia. *Nat Rev Dis Primers*. 2017;3(1):17008.

3. Brown JR. How I treat CLL patients with ibrutinib. *Blood*. 2018;131(4):379-386.

4. Carmier D, Dartigeas C, Mankikian J, et al. Serious bronchopulmonary involvement due to chronic lymphocytic leukaemia. *Eur Respir Rev*. 2013;22(129): 416-419.

5. Ahmed S, Siddiqui AK, Rossoff L, Sison CP, Rai KR. Pulmonary complications in chronic lymphocytic leukemia. *Cancer*. 2003;98(9):1912-1917.

6. Korona-Glowniak I, Grywalska E, Grzegorczyk A, Roliński J, Glowniak A, Malm A. Bacterial colonization in patients with chronic lymphocytic leukemia and factors associated with infections and colonization. *J Clin Med*. 2019;8(6):E861.

7. Itälä M, Helenius H, Nikoskelainen J, Remes K. Infections and serum IgG levels in patients with chronic lymphocytic leukemia. *Eur J Haematol*. 1992; 48(5):266-270.

8. Rossi D, De Paoli L, Rossi FM, et al. Early stage chronic lymphocytic leukaemia carrying unmutated IGHV genes is at risk of recurrent infections during watch and wait. *Br J Haematol*. 2008;141(5):734-736.

9. Forconi F, Moss P. Perturbation of the normal immune system in patients with CLL. *Blood*. 2015;126(5):573-581.

10. Morrison VA. Infectious complications of chronic lymphocytic leukaemia: pathogenesis, spectrum of infection, preventive approaches. *Best Pract Res Clin Haematol*. 2010;23(1):145-153.

11. Dearden C. Disease-specific complications of chronic lymphocytic leukemia. *Hematology Am Soc Hematol Educ Program*. 2008;2008:450-456.

12. Morrison VA. Management of infectious complications in patients with chronic lymphocytic leukemia. *Hematology Am Soc Hematol Educ Program*. 2007;2007:332-338.

13. Wadhwa PD, Morrison VA. Infectious complications of chronic lymphocytic leukemia. *Semin Oncol*. 2006;33(2):240-249.

14. Tsiodras S, Samonis G, Keating MJ, Kontoyiannis DP. Infection and immunity in chronic lymphocytic leukemia. *Mayo Clin Proc*. 2000;75(10):1039-1054.

15. Foxman B. Epidemiology of urinary tract infections: incidence, morbidity, and economic costs. *Dis Mon*. 2003;49(2):53-70.

16. Ulett GC, Totsika M, Schaale K, Carey AJ, Sweet MJ, Schembri MA. Uropathogenic Escherichia coli virulence and innate immune responses during urinary tract infection. *Curr Opin Microbiol*. 2013;16(1):100-107.

17. Mulvey MA, Lopez-Boado YS, Wilson CL, et al. Induction and evasion of host defenses by type 1-piliated uropathogenic Escherichia coli. *Science*. 1998; 282(5393):1494-1497.

18. Nosari A. Infectious complications in chronic lymphocytic leukemia. *Mediterr J Hematol Infect Dis*. 2012;4(1):e2012070.

19. Agace WW, Hedges SR, Ceska M, Svanborg C. Interleukin-8 and the neutrophil response to mucosal gram-negative infection. *J Clin Invest*. 1993;92(2): 780-785.

20. Bottek J, Soun C, Lill JK, et al. Spatial proteomics revealed a CX$_3$CL1-dependent crosstalk between the urothelium and relocated macrophages through IL-6 during an acute bacterial infection in the urinary bladder. *Mucosal Immunol*. 2020;13(4):702-714.

21. Schiwon M, Weisheit C, Franken L, et al. Crosstalk between sentinel and helper macrophages permits neutrophil migration into infected uroepithelium. *Cell*. 2014;156(3):456-468.

22. Abraham SN, Miao Y. The nature of immune responses to urinary tract infections. *Nat Rev Immunol*. 2015;15(10):655-663.

23. Svensson M, Yadav M, Holmqvist B, Lutay N, Svanborg C, Godaly G. Acute pyelonephritis and renal scarring are caused by dysfunctional innate immunity in mCxcr2 heterozygous mice. *Kidney Int*. 2011;80(10):1064-1072.

24. Podaza E, Sabbione F, Risnik D, et al. Neutrophils from chronic lymphocytic leukemia patients exhibit an increased capacity to release extracellular traps (NETs). *Cancer Immunol Immunother*. 2017;66(1):77-89.

25. Itälä M, Vainio O, Remes K. Functional abnormalities in granulocytes predict susceptibility to bacterial infections in chronic lymphocytic leukaemia. *Eur J Haematol*. 1996;57(1):46-53.

26. Zeya HI, Keku E, Richards F II, Spurr CL. Monocyte and granulocyte defect in chronic lymphocytic leukemia. *Am J Pathol*. 1979;95(1):43-54.

27. Kontoyiannis DP, Georgiadou SP, Wierda WG, et al. Impaired bactericidal but not fungicidal activity of polymorphonuclear neutrophils in patients with chronic lymphocytic leukemia. *Leuk Lymphoma*. 2013;54(8):1730-1733.

28. Manukyan G, Papajik T, Gajdos P, et al. Neutrophils in chronic lymphocytic leukemia are permanently activated and have functional defects. *Oncotarget*. 2017;8(49):84889-84901.

29. Podaza E, Risnik D, Colado A, et al. Chronic lymphocytic leukemia cells increase neutrophils survival and promote their differentiation into CD16(high) CD62L(dim) immunosuppressive subset. *Int J Cancer*. 2019;144(5):1128-1134.

30. Bichi R, Shinton SA, Martin ES, et al. Human chronic lymphocytic leukemia modeled in mouse by targeted TCL1 expression. *Proc Natl Acad Sci USA*. 2002;99(10):6955-6960.

31. McClanahan F, Hanna B, Miller S, et al. PD-L1 checkpoint blockade prevents immune dysfunction and leukemia development in a mouse model of chronic lymphocytic leukemia. *Blood*. 2015;126(2):203-211.

32. Hanna BS, McClanahan F, Yazdanparast H, et al. Depletion of CLL-associated patrolling monocytes and macrophages controls disease development and repairs immune dysfunction in vivo. *Leukemia*. 2016;30(3):570-579.

33. Öztürk S, Roessner PM, Schulze-Edinghausen L, et al. Rejection of adoptively transferred Eμ-TCL1 chronic lymphocytic leukemia cells in C57BL/6 substrains or knockout mouse lines. *Leukemia*. 2019;33(6):1514-1539.

34. Engel D, Dobrindt U, Tittel A, et al. Tumor necrosis factor alpha- and inducible nitric oxide synthase-producing dendritic cells are rapidly recruited to the bladder in urinary tract infection but are dispensable for bacterial clearance. *Infect Immun*. 2006;74(11):6100-6107.

35. Engel DR, Maurer J, Tittel AP, et al. CCR2 mediates homeostatic and inflammatory release of Gr1(high) monocytes from the bone marrow, but is dispensable for bladder infiltration in bacterial urinary tract infection. *J Immunol*. 2008;181(8):5579-5586.

36. Berger H, Hacker J, Juarez A, Hughes C, Goebel W. Cloning of the chromosomal determinants encoding hemolysin production and mannose-resistant hemagglutination in *Escherichia coli*. *J Bacteriol*. 1982;152(3):1241-1247.

37. Dixit A, Bottek J, Beerlage AL, et al. Frontline science: proliferation of ly6c$^+$ monocytes during urinary tract infections is regulated by IL-6 trans-signaling. *J Leukoc Biol*. 2018;103(1):13-22.

38. Pohl JM, Volke JK, Thiebes S, et al. CCR2-dependent Gr1^{high} monocytes promote kidney injury in shiga toxin-induced hemolytic uremic syndrome in mice. *Eur J Immunol*. 2018;48(6):990-1000.

39. Pohl JM, Gutweiler S, Thiebes S, et al. *Irf4*-dependent CD103$^+$CD11b$^+$ dendritic cells and the intestinal microbiome regulate monocyte and macrophage activation and intestinal peristalsis in postoperative ileus. *Gut*. 2017;66(12):2110-2120.

40. Zec K, Volke J, Vijitha N, et al. Neutrophil migration into the infected uroepithelium is regulated by the crosstalk between resident and helper macrophages. *Pathogens*. 2016;5(1):E15.

41. Engel DR, Krause TA, Snelgrove SL, et al. CX3CR1 reduces kidney fibrosis by inhibiting local proliferation of profibrotic macrophages. *J Immunol*. 2015; 194(4):1628-1638.

42. Witzke KE, Großerueschkamp F, Jütte H, et al. Integrated Fourier transform infrared imaging and proteomics for identification of a candidate histochemical biomarker in bladder cancer. *Am J Pathol*. 2019;189(3):619-631.

43. Pearson K. On the criterion that a given system of deviations from the probable in the case of a correlated system of variables is such that it can be reasonably supposed to have arisen from random sampling. *Philos Mag*. 1900;50(302):157-175.

44. Hastie T, Tibshirani R, Friedman J, Franklin J. *The Elements of Statistical Learning: Data Mining, Inference, and Prediction (Second Edition)*. New York: Springer; 2009.

45. Benjamini Y, Hochberg Y. Controlling the false discovery rate - a practical and powerful approach to multiple testing. *J R Stat Soc Series B Stat Methodol*. 1995;57(1):289-300.

46. Breiman L. Random forests. *Mach Learn*. 2001;45(1):5-32.

47. Bardoel BW, Kenny EF, Sollberger G, Zychlinsky A. The balancing act of neutrophils. *Cell Host Microbe*. 2014;15(5):526-536.

48. von Mering C, Jensen LJ, Snel B, et al. STRING: known and predicted protein-protein associations, integrated and transferred across organisms. *Nucleic Acids Res.* 2005;33(Database issue):D433-D437.

49. Eash KJ, Greenbaum AM, Gopalan PK, Link DC. CXCR2 and CXCR4 antagonistically regulate neutrophil trafficking from murine bone marrow. *J Clin Invest.* 2010;120(7):2423-2431.

50. Chapman AL, Mocatta TJ, Shiva S, et al. Ceruloplasmin is an endogenous inhibitor of myeloperoxidase. *J Biol Chem.* 2013;288(9):6465-6477.

51. Kolaczkowska E, Kubes P. Neutrophil recruitment and function in health and inflammation. *Nat Rev Immunol.* 2013;13(3):159-175.

52. Zhang D, Chen G, Manwani D, et al. Neutrophil ageing is regulated by the microbiome. *Nature.* 2015;525(7570):528-532.

53. Kolaczkowska E. The older the faster: aged neutrophils in inflammation. *Blood.* 2016;128(19):2280-2282.

54. Ferri LE, Chia S, Benay C, Giannias B, Christou NV. L-selectin shedding in sepsis limits leukocyte mediated microvascular injury at remote sites. *Surgery.* 2009;145(4):384-391.

55. Eruslanov EB, Bhojnagarwala PS, Quatromoni JG, et al. Tumor-associated neutrophils stimulate T cell responses in early-stage human lung cancer. *J Clin Invest.* 2014;124(12):5466-5480.

56. Deniset JF, Surewaard BG, Lee WY, Kubes P. Splenic Ly6G^high mature and Ly6G^int immature neutrophils contribute to eradication of *S. pneumoniae. J Exp Med.* 2017;214(5):1333-1350.

57. Frelin C, Ofran Y, Ruston J, et al. Grb2 regulates the proliferation of hematopoietic stem and progenitors cells. *Biochim Biophys Acta Mol Cell Res.* 2017; 1864(12):2449-2459.

58. Leliefeld PHC, Pillay J, Vrisekoop N, et al. Differential antibacterial control by neutrophil subsets. *Blood Adv.* 2018;2(11):1344-1355.

59. Ivetic A. A head-to-tail view of L-selectin and its impact on neutrophil behaviour. *Cell Tissue Res.* 2018;371(3):437-453.

60. Spiller F, Costa C, Souto FO, et al. Inhibition of neutrophil migration by hemopexin leads to increased mortality due to sepsis in mice. *Am J Respir Crit Care Med.* 2011;183(7):922-931.

61. Pylaeva E, Lang S, Jablonska J. The essential role of type I interferons in differentiation and activation of tumor-associated neutrophils. *Front Immunol.* 2016;7:629.

62. Futosi K, Fodor S, Mócsai A. Reprint of neutrophil cell surface receptors and their intracellular signal transduction pathways. *Int Immunopharmacol.* 2013;17(4):1185-1197.

63. King KY, Baldridge MT, Weksberg DC, et al. Irgm1 protects hematopoietic stem cells by negative regulation of IFN signaling. *Blood.* 2011;118(6): 1525-1533.

64. Azzam KM, Madenspacher JH, Cain DW, et al. Irgm1 coordinately regulates autoimmunity and host defense at select mucosal surfaces. *JCI Insight.* 2017;2(16):91914.

65. Bafica A, Feng CG, Santiago HC, et al. The IFN-inducible GTPase LRG47 (Irgm1) negatively regulates TLR4-triggered proinflammatory cytokine production and prevents endotoxemia. *J Immunol.* 2007;179(8):5514-5522.

66. Tomic J, Lichty B, Spaner DE. Aberrant interferon-signaling is associated with aggressive chronic lymphocytic leukemia. *Blood.* 2011;117(9):2668-2680.

67. Li C, Wang J, Zhang H, et al. Interferon-stimulated gene 15 (ISG15) is a trigger for tumorigenesis and metastasis of hepatocellular carcinoma. *Oncotarget.* 2014;5(18):8429-8441.

68. Sainz B Jr., Martín B, Tatari M, Heeschen C, Guerra S. ISG15 is a critical microenvironmental factor for pancreatic cancer stem cells. *Cancer Res.* 2014; 74(24):7309-7320.

69. Chen RH, Du Y, Han P, et al. ISG15 predicts poor prognosis and promotes cancer stem cell phenotype in nasopharyngeal carcinoma. *Oncotarget.* 2016; 7(13):16910-16922.

70. Swaim CD, Scott AF, Canadeo LA, Huibregtse JM. Extracellular ISG15 signals cytokine secretion through the LFA-1 integrin receptor. *Mol Cell.* 2017; 68(3):581-590.e5.

71. Spaner DE, McCaw L, Wang G, Tsui H, Shi Y. Persistent janus kinase-signaling in chronic lymphocytic leukemia patients on ibrutinib: results of a phase I trial. *Cancer Med.* 2019;8(4):1540-1550.

72. Jain P, Keating M, Renner S, et al. Ruxolitinib for symptom control in patients with chronic lymphocytic leukaemia: a single-group, phase 2 trial. *Lancet Haematol.* 2017;4(2):e67-e74.